Available online at www.sciencedirect.com
SCIENCE DIRECT®
Biomaterials 27 (2006) 2507–2517
Biomaterials
www.elsevier.com/locate/biomaterials

Age, dehydration and fatigue crack growth in dentin

Devendra Bajaj, Naryana Sundaram, Ahmad Nazari, D. Arola*

Department of Mechanical Engineering, University of Maryland Baltimore County, 1000 Hilltop Circle, Baltimore, MD 21250, USA

Received 9 October 2005; accepted 17 November 2005
Available online 9 December 2005

Abstract

A preliminary study of the effects from age and dehydration on fatigue crack growth in human dentin was conducted. Compact tension (CT) fatigue specimens of coronal dentin were prepared from extracted molars and subjected to high cycle fatigue ($10^5 < N < 10^6$) under Mode I loading. Young hydrated dentin (mean age = 25 ± 7 years), old hydrated dentin (mean age = 55 ± 14 years) and young dehydrated dentin (mean age = 20 ± 2 years) were examined. Fatigue crack growth rates were quantified according to the Paris Law in terms of the crack growth exponent (m) and coefficient (C). The average fatigue crack growth exponent for the young hydrated dentin ($m = 13.3 \pm 1.1$) was significantly less than that for the hydrated old ($m = 21.6 \pm 5.2$; $p < 0.003$) and dehydrated young dentin ($m = 18.8 \pm 2.8$; $p < 0.01$). Fatigue cracks in the old dentin underwent initiation at a lower stress intensity range than in young dentin and propagated at as significantly faster rate (over 100 ×). Differences in the microscopic features of the fracture surfaces from the old and young dentin suggested that particular mechanisms contributing to energy dissipation and crack growth resistance in the young hydrated dentin were not present in the old dentin. Based on results of this study, the fatigue crack growth resistance of human dentin decreases with both age of the tissue and dehydration.

Keywords: Age; Dentin; Fatigue; Fracture toughness

1. Introduction

The many advances in preventive and restorative dentistry have resulted in a general decline in the incidence of dental caries, especially in children. With this increase in quality of oral health, it is envisioned that the number of fully dentate adults will continue to rise [1]. In fact, there has been a steady decline in edentulism since the 1960s [2]. Seniors are now seeking restorative care more frequently and this group of patients brings about a new set of oral health problems. Senior patients have a larger number of restored teeth, and these are generally at a greater risk of recurrent decay or fracture. For example, the occurrence of both crown and root caries has been reported to be as high as 65% in patients exceeding 65 years of age [3–5]. In the United Kingdom, it was recently found that 50% of the teeth of dentate adults aged 45 years and over are filled or crowned [6]. Therefore, in spite of a decrease in caries in the young, new restorations and repairs of existing restorations are likely to be required just as regularly, but now in an older group of patients. This trend has been identified in both the United States and Europe [7–9].

Current restorative techniques may not be as successful on older teeth due to specific structural changes that take place with aging. One of the most marked changes occurs in dentin, the hard tissue occupying the majority of the tooth by both weight and volume. The dentin is traversed by a network of tubules that extend radially outward between the pulp and dentin-enamel junction (DEJ). With age there is a gradual occlusion of the dentin tubules due to deposition of mineral within the lumen. After a sufficient degree of occlusion the tissue appears transparent and dentin that has undergone this change is regarded as "sclerotic" [10,11]. Bonding to sclerotic dentin is hampered by difficulties in demineralization [12–15], and consequent development of inferior resin tags. In fact, the bonding strength to sclerotic dentin is significantly lower than that in bonding to normal dentin [16,17]. Age-related structural

*Corresponding author. Tel.: +1 (410) 455 3310; fax: +1 (410) 455 1052.
E-mail address: darola@umbc.edu (D. Arola).

0142-9612/$ - see front matter © 2005 Elsevier Ltd. All rights reserved.
doi:10.1016/j.biomaterials.2005.11.035

changes in dentin may also be detrimental to the mechanical properties of this tissue.

Comparisons of the structure and chemistry of normal and sclerotic dentin have been reported. Using spectroscopy and fluorescence microscopy, Balooch et al. [18] studied the intertubular and peritubular components of human dentin and identified differences in chemistry between normal and sclerotic dentin. The deposited material filling the tubules in sclerotic dentin appeared to be a less dense form of apatite, and reminiscent of the peritubular dentin. Kinney et al. [19] and Porter et al. [20] adopted a host of advanced techniques in evaluating the structure and chemistry of sclerotic dentin. According to these studies the mineral concentration of sclerotic dentin is significantly higher than that of normal dentin and the chemistry of the deposited material (within the lumen) is consistent with that of the intertubular dentin. Thus, the higher mineral content is attributed to the mineral deposits within the lumens. Both studies distinguished that there was a reduction in crystal size in the intertubular sclerotic dentin relative to normal dentin. Based on the chemistry of the deposited mineral within the lumen and changes in crystal size a "dissolution and precipitation" mechanism was proposed responsible for occlusion of the tubules and formation of sclerotic dentin. It is unclear whether these transformations are sufficient to elicit differences in the mechanical properties of dentin as well.

Very few studies have evaluated the contribution from aging to the mechanical properties of dentin. Earlier studies have focused on the hydration of dentin and effects on the mechanical properties. In an evaluation of moisture content, teeth over 50-year old reportedly contained less water than young teeth (10–20 years of age) [21]. Dehydrated dentin has lower toughness [22–24], and has been described as being brittle [25]. If dehydration serves as an adequate model for evaluating the effects of aging and formation of sclerotic dentin, results of these studies imply that dentin undergoes a reduction in toughness with aging. Tonami and Takahashi [26] examined the effects of aging on bovine dentin and found that the fatigue strength of dentin from young animals was greater than that of the adults. Yet, the difference in age between the two groups of animals was limited to only a few years. Using nanoindentation, Balooch et al. [18] found that the elastic modulus and hardness of the intertubular and peritubular components were essentially equivalent in normal and sclerotic dentin and the hardness of the deposited material within the lumens was between that for the intertubular and peritubular dentin. Meanwhile, Kinney et al. [19] found that while there was no significant difference in the elastic modulus or hardness between sclerotic and normal dentin, the fracture toughness of the sclerotic dentin was approximately 20% lower than that of normal dentin and the sclerotic dentin exhibited an inferior fatigue life. A recent study by the authors distinguished that the fatigue strength of human coronal dentin from older patients ($50 \leqslant$ age $\leqslant 80$) was significantly lower than that of young patients ($17 \leqslant$ age $\leqslant 30$) [27]. In fact, the apparent endurance strength of "old" dentin was only half that of the dentin from young patients.

Fatigue failure of restored teeth is undoubtedly a function of the stress-life behavior (comprising mostly the initiation of damage) and fatigue crack growth [28,29]. Thus, results from the aforementioned studies suggest that dentin may undergo a reduction in resistance to fatigue crack growth with age. As flaws may be introduced during the restorative process, it is necessary to identify the significance of age and hydration on fatigue crack growth in dentin. In this investigation, the fatigue crack growth properties of human dentin were evaluated. The primary objective of the study was to identify if age and/or dehydration contributed to the rate of fatigue crack growth and mechanisms of cyclic extension.

2. Materials and methods

Second and third molars were obtained from dental practices in Maryland according to an approved protocol issued by the Institutional Review Board of the University of Maryland. Immediately after extraction the teeth were placed in Hank's balanced salt solution (HBSS) and stored with record of the age and gender. Non-carious molars were selected, molded in a polymer resin and sectioned using a numerical controlled slicer/grinder under water-based coolant. Diamond abrasive slicing wheels were used to obtain mesial-distal or buccal-lingual sections from the selected molars (Fig. 1(a)). Secondary sections were then introduced to obtain compact tension (CT) specimens with overall

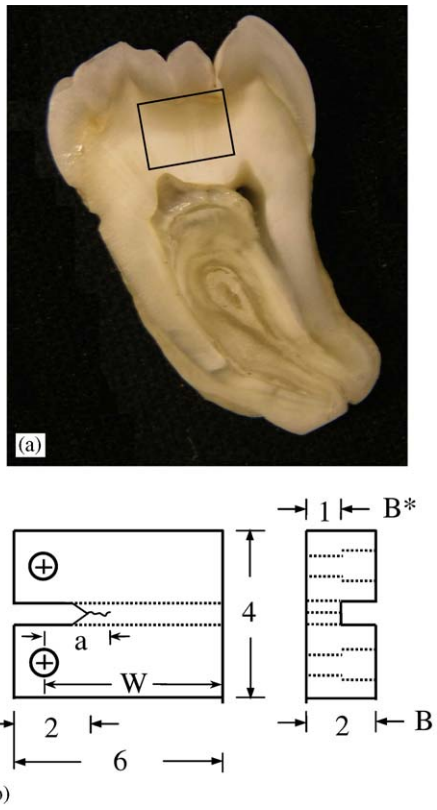

Fig. 1. A dentin CT specimen machined from a human 3rd molar: (a) a section and possible specimen; (b) final geometry of the CT specimens.

geometry conforming to ASTM standard E647 [30] for fatigue crack growth. Precision holes were introduced using a miniature milling machine to enable application of opening mode (Mode I) loads. The notch tip of each specimen was sharpened using a razor blade and 1 μm diamond paste to facilitate stable crack initiation. The process resulted in a notch-tip radius of approximately 20 μm. A schematic diagram of the specimen geometry with identification of critical features is shown Fig. 1(b).

Fatigue crack growth properties of the human dentin were determined as a function of the patient age and hydration. At receipt the molars were divided into two age groups corresponding to "young" ($17 \leqslant \text{age} \leqslant 35$) and "old" ($47 \leqslant \text{age}$). The two age groups were established primarily according to the age distribution of molars received and were not based on specific external or microscopic features of the tubules. The age groups are reasonably consistent with trends identified in a previous study on the mechanical behavior of dentin under quasi-static and fatigue flexure. Results from that study indicated that the properties of dentin from the teeth of patients with age $\geqslant 50$ appeared to be consistent and could be characterized as "old" [27]. In examination of the sectioned molars within the older age group of the present study, some had clearly visible regions of sclerosis, particularly in the roots. However, not all the molars exhibited regions of sclerotic dentin, and few had sclerosis extending within the coronal dentin where the CT specimens were obtained. Consequently, the patient age was used for classification and appeared to provide the most objective description.

A total of 22 dentin CT specimens were prepared including 9 hydrated specimens from young patients (avg. age $\pm$ std. dev. $= 25 \pm 7$), 8 hydrated specimens from old patients (55 ± 14) and 5 specimens from young patients that were fully dehydrated (20 ± 2). Fatigue crack growth in the hydrated specimens was conducted with the specimens immersed in an HBSS bath at room temperature (22 °C). Dehydration was achieved using a free convection tissue drying oven (Blue M Model OV-12A) at 60 °C and the process was monitored using weight measurements until the specimens reached steady state as confirmed by 3 successive intervals of hydration without changes in weight. The dehydration process required 5 h or more and the average decrease in weight was $4.94 \pm 0.82\%$. Fatigue crack growth testing of the dehydrated specimens was initiated immediately following dehydration.

Following preparation, the dentin specimens were subjected to fatigue loads using an Enduratec Model 3200 universal testing system, which has a maximum load capacity and sensitivity of 225 and ± 0.01 N, respectively. All hydrated specimens (young and old) underwent cyclic loading in an HBSS bath (22 °C) while the dehydrated specimens were loaded in air without environment control. Fatigue loading of the specimens was achieved under load actuation at 5 Hz using a cyclic stress ratio (R) of 0.1; assuming linear-elastic response, the ratio of the minimum and maximum load are 0.1 as well. The load was applied in opening mode (Mode I) and administered by stainless steel pins placed within the holes of the specimen (Fig. 2(a)). Note that the holes were counterbored from the back side (side of channel) to a depth consistent with the remaining ligament thickness (Fig. 1(b)), which insured that the resolved opening mode load was applied through the center of the ligament thickness. Prior to cyclic loading the front face of each specimen was stained with an indelible marker to improve contrast between the crack and dentin. Crack length measurements were conducted visually using a back lighting technique in which the back surface (with channel) was illuminated with white light and inspection of the crack length occurred on the stained face. Owing to the partially transparent nature of dentin, the transmitted light underwent diffraction on the crack face and resulted in illumination of the crack tip (Fig. 2(b)). Crack initiation at the notch tip was achieved through application of a cyclic load with maximum load of approximately 14 N. Initiation of a crack from the notch tip was typically evident from a change in the displacement history of the specimens due to an increase in compliance. Inspection of the notch tip or crack length was conducted using an optical microscope (100 ×) with scaled reticule. After identification of a well-defined crack at the notch tip, the crack was extended approximately 0.5 mm prior to beginning the incremental crack length measurements to preclude stress gradient effects from the notch. During this period of extension the load was reduced to a maximum load of between 8 and 14 N according to the crack length and relative rate of cyclic extension observed after initiation. The maximum cyclic load remained constant at this value (after initiation) throughout all regions of extension. Measurements of the change in crack length ($\Delta a = (a_{i+1} + a_i)/2$) were made over specific intervals of fatigue loading until complete specimen fracture. The number of cycles between measurements (ΔN) was chosen according to the observed crack growth rate and typically ranged between 10 and 25 kcycles. For an overall average growth rate of 1.0E-05 mm/cycle, the average increment of extension was between 100 and 300 μm. To help identify the crack tip during visual observations the specimen was subjected to cyclic loading at 1 Hz using the same stress ratio and maximum load. Crack lengths could also be estimated using the compliance approach [30] according to the magnitude of opening displacement and the specimen geometry. However, dentin exhibits toughening behavior with crack extension (i.e. R-curve behavior) due to both intrinsic and extrinsic mechanisms [24,31,32]. Therefore, crack length estimates based on compliance would be subject to error and potential differences in the mechanisms of crack growth resistance with dehydration and age would cause inconsistent error between the three groups of specimens.

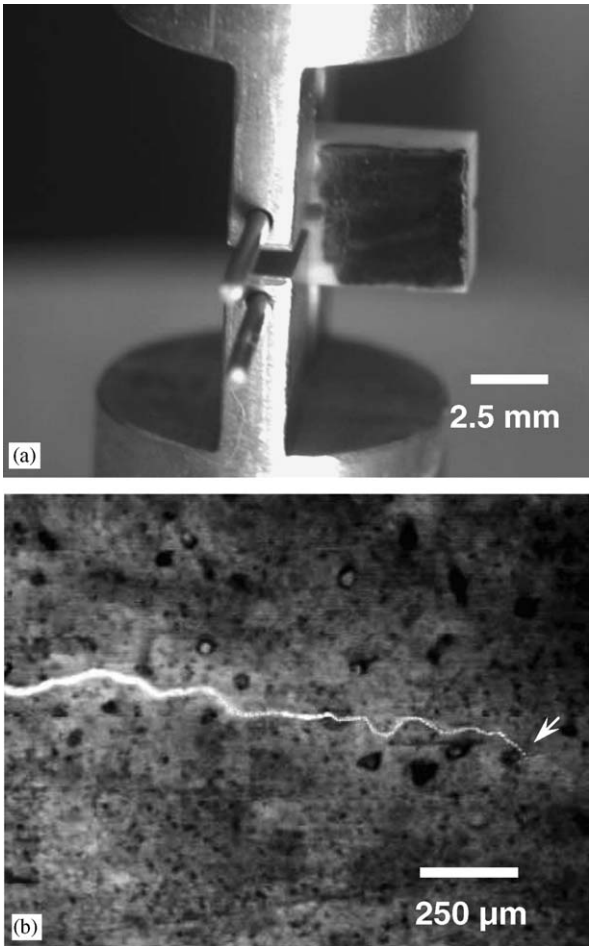

Fig. 2. Fatigue loading and back illumination: (a) a CT specimen within the load fixture; (b) back illumination of a crack (arrow indicates tip).

Using the incremental crack length measurements corresponding to the steady state (Region II) response, the fatigue crack growth rate (da/dN) was quantified using the Paris Law [33] according to

$$\frac{da}{dN} = C(\Delta K)^m, \tag{1}$$

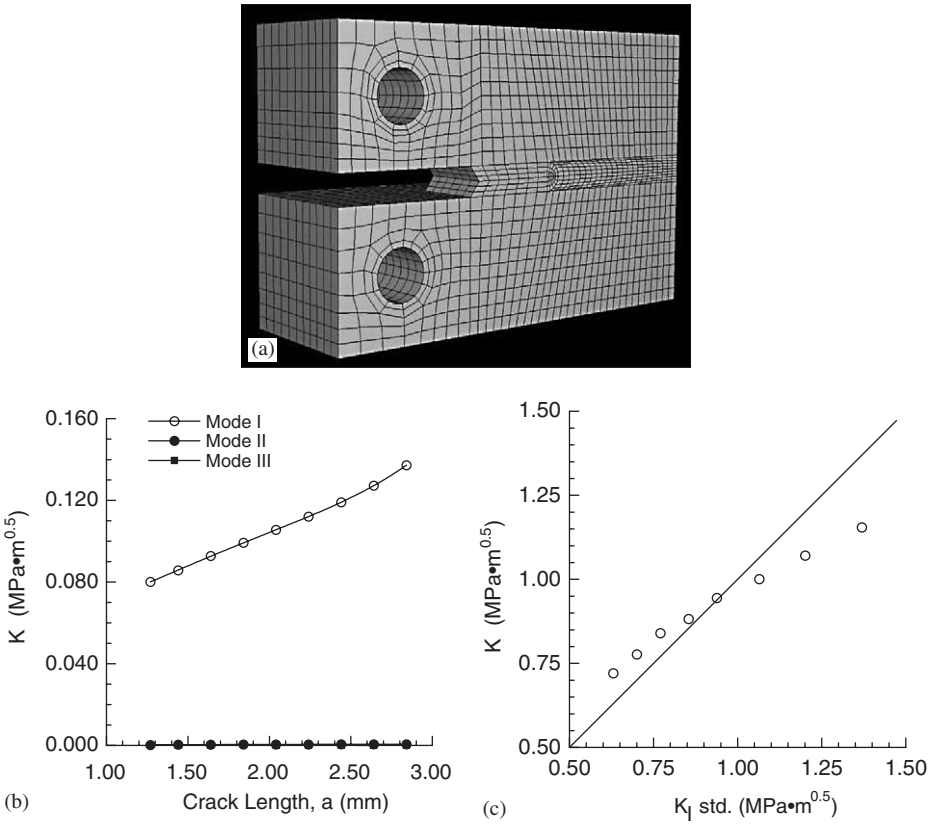

Fig. 3. The finite element model for the modified CT specimens used for evaluating fatigue crack growth in dentin and the stress intensity distribution: (a) the finite element model for the dentin CT specimens; (b) distribution of the stress intensity with crack length in the CT specimens as estimated from the numerical analysis. Note that the stress intensity has been obtained for an opening mode load (P) of unity; (c) comparison of the stress intensity estimated from the standard (ASTM E647 [30]) with the actual stress intensity for the dentin CT specimens determined using the finite element model.

where ΔK is the stress intensity range, and da and dN represent the incremental crack extension (Δa) and number of cycles (ΔN), respectively. The quantities C and m are the fatigue crack growth coefficient and exponent, respectively, while the stress intensity range (ΔK) is determined from the difference in stress intensity at the minimum and maximum loads. For CT specimens with geometry abiding by ASTM standard E647 [30] the stress intensity at the crack tip (K) can be estimated according to

$$K = \frac{P}{B\sqrt{W}}\frac{(2+\alpha)}{(1-\alpha)^{3/2}}(0.886 + 4.64\alpha - 13.32\alpha^2 + 14.72\alpha^3 - 5.6\alpha^4), \quad (2)$$

where, P is the maximum opening load, B the specimen thickness, and W the distance between point of load application and free boundary (Fig. 1(b)). The quantity α is equal to the ratio of the average crack length over the growth increment ($(a_{i+1} + a_i)/2$) to W.

Preliminary experiments showed that crack-curving occurred in specimens with specific tubule orientations. In general, the CT specimens in the present study were prepared such that the tubules were oriented perpendicular to the plane of crack growth, i.e. the orientation with lowest fracture toughness [32,34]. Previous studies conducted with bovine dentin have shown that the fatigue crack growth is dependent on tubule orientation [35]. According to these concerns, a back-channel was introduced in the dentin CT specimens (Fig. 1(b)) to guide the direction of crack extension and maintain growth along the plane of maximum normal stress. A channel is more often introduced on both faces to maintain symmetry, but was not employed for the dentin specimens due to difficulties in identifying the crack tip within the small channel and due to moisture remaining within channel after draining the hydration bath. It is also important to highlight that activities of the present investigation were part of a much larger investigation concerning variation in tubule orientation. Thus, all specimens were prepared with back channel. According to ASTM E647, the required specimen thickness (B) for evaluating fatigue crack growth ranges from $W/20 \leqslant B \leqslant W/4$. The average ligament thickness from the front face to the channel base was 1.0 mm. Thus, the specimen thickness within the channel region complied with the required range.

Differences in size of the dentin CT specimens with relation to ASTM standard E647 and additional modifications of the geometry potentially limited validity of Eq. (2) for estimating ΔK. Owing to these concerns a numerical model was developed to determine the stress intensity distribution within the modified CT specimens as a function of crack length, channel depth and opening load. A 3-D finite element model was developed for the dentin CT specimen geometry (Fig. 1(b)) using commercially available software.[1] The model consisted of nearly 11,000 20-noded 2nd order brick elements (C3D20) with reduced integration points. A refined mesh was used near the crack tip to account for the stress gradient posed by the crack (Fig. 3(a)). To achieve square root singularity in the stress and strain distribution, the crack tip was modeled using a ring of second-order brick elements with collapsed face, and biased node placement towards the crack tip. The collapsed crack tip elements were treated as infinite elements according to the approach of Zienkiewicz et al. [36]. The dentin was treated as linear elastic and isotropic with elastic modulus of 19 GPa and Poission's ratio of 0.3, which are within the range of reported values for these properties [37].

The stress intensity distribution was estimated in terms of the energy release rate with crack extension. Crack growth in the numerical model was simulated using a "virtual" crack extension feature available from the commercial software. Several contours were selected around the crack tip to estimate the energy released with crack extension. Numerical solutions

[1] ABAQUS; Version 6.5.

of the stress intensity can be influenced by the selection of nodes adjacent to the crack tip and according to the size of the K-dominant region. Thus, a series of contours were defined about the crack and the contour integrals that provided a uniform estimate of the energy released with extension were selected. The energy release rate and corresponding stress intensity were determined from the average of a minimum of five contour integrals defined about the crack tip. In Mode I the relationship between the energy release rate and the corresponding stress intensity is described by [38]

$$G = \frac{1}{\bar{E}} K_I^2, \tag{3}$$

where $\bar{E} = E/(1-\nu^2)$ for plane strain. Note that counterboring of the holes to a depth equivalent to the channel depth (Fig. 1(b)) resulted in symmetric load distribution about the ligament centerline and maintained Mode I loading. However, a stress concentration is posed by the back channel geometry, which promotes an increase in the opening mode stress near the channel root. To insure that the geometric changes of the dentin CT specimens did not cause mixed mode loading all three components of the stress intensity (i.e. K_I, K_{II}, and K_{III})) were quantified using the numerical model.

The stress intensity distribution was evaluated across the specimen thickness, and as a function of the crack length from $1.5\,\text{mm} \leqslant a \leqslant 3\,\text{mm}$. The stress intensity distribution with crack extension is shown for all three modes (i.e. I, II, and III) in Fig. 3(b); the magnitude of each K has been normalized by the opening load (P). Both the in-plane and out-of-plane shearing components (K_{II} and K_{III}) were found to be at least two orders of magnitude lower than Mode I. Using a non-linear least-squares error approximation for K with respect to crack length and specimen geometry, the distribution in K_I with crack extension for the modified CT specimens is given by

$$K_I = \frac{P}{B^*\sqrt{W}} \left(\frac{B^*+1}{B+1}\right)^{0.5} (0.131 + 0.320\,\alpha + 0.211\,\alpha^2), \tag{4}$$

where P is the load, the α the ratio of a to W (Fig. 1(b)) and the quantities $B*$ and B are the ligament thickness (within the region of the channel) and nominal specimen thickness, respectively; the parameters defining geometry in Eq. (4) are listed in mm. Note that the distribution in K described by Eq. (4) provides the average across the specimen's thickness. The relationship between K_I estimated using ASTM E647 (Eq. (2)) and K_I estimated using Eq. (4) is shown in Fig. 3(c). According to these results, the stress intensity for the modified CT specimen estimated using Eq. (2) would be within 20% of the actual stress intensity determined using the FEM. Nevertheless, the stress intensity range for all CT specimens was estimated from the crack length measurements using Eq. (4).

Using the incremental crack length measurements and the corresponding stress intensity (Eq. (4)), the fatigue crack growth rate (da/dN) was plotted in terms of ΔK to estimate the quantities m and C for each specimen. A power law trend-line was fit to the steady state region (Region II) of crack growth to obtain least-squares error estimates for C and m. A comparison of the fatigue crack growth parameters was conducted using the Student's t-test to establish differences in the mean and variance, respectively.

Since the orientation of the dentin tubules was not known prior to cyclic loading visual measurements of tubule angles were made after fracture of the specimens using a JEOL Model JSM-5600 scanning electron microscope (SEM) in the secondary electron imaging (SEI) mode. To enhance conductance of the fracture surface, the fractured CT specimens were sputtered with gold palladium. Finally, the fracture surface morphology was examined to establish differences in the mechanisms of fatigue crack growth associated with hydration or age.

3. Results

A representative fatigue crack growth response for a young hydrated dentin specimen is shown in Fig. 4 and exhibits the three characteristic regions of fatigue crack growth. The Paris Law exponent (m) and coefficient (C) for

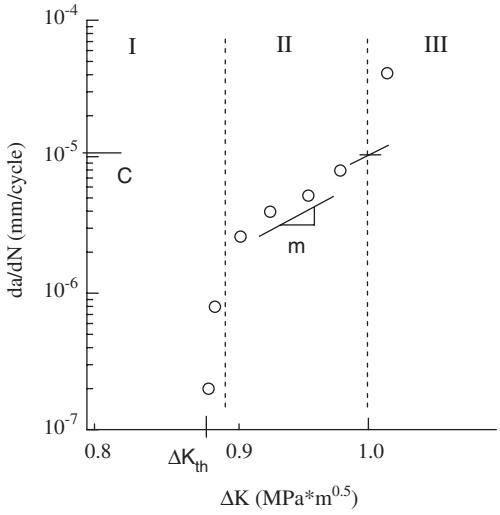

Fig. 4. A typical fatigue crack growth response distinguishing all three regions of cyclic extension and the Paris Law parameters.

Region II growth are highlighted in this figure for clarity. The stress intensity threshold (ΔK_{th}) is also distinguished which defines a critical stress intensity below which fatigue crack growth is presumed not to occur. Overall, fatigue crack growth rates in the dentin specimens ranged from approximately 1E-7 to 5E-3 mm/cycle. Not all specimens exhibited the three regions of crack growth highlighted in Fig. 4. In general, the young hydrated dentin specimens exhibited all three regions, whereas the dehydrated and old dentin specimens did not exhibit a clear region of initiation, nor a strong transition from steady state (Region II) to unstable (Region III) growth. In general, the number of cycles required for crack initiation and growth in the old dentin and dehydrated young dentin took much less time than in the hydrated young dentin.

The Region II crack growth responses were identified and are shown for all the dentin specimens in Fig. 5(a). As evident in this figure, fatigue crack growth in the old and dehydrated dentin occurred at a lower stress intensity range than the young hydrated dentin. The Paris Law parameters for each of the young hydrated dentin are listed in Table 1 along with the average exponent and coefficient; note that the average coefficient (C) was estimated from the antilog of the average of ($\log(C)$). Similarly, the growth parameters for the old hydrated dentin and dehydrated young dentin are listed in Table 2 and 3, respectively. The average Paris Law exponents of the old dentin ($m = 21.6 \pm 5.2$; $p < 0.003$) and dehydrated dentin ($m = 18.8 \pm 2.8$; $p < 0.01$) were significantly greater than that of the young hydrated dentin ($m = 13.3 \pm 1.1$). The larger fatigue crack growth exponent for the old and dehydrated dentin indicates that fatigue crack growth in these tissues was more sensitive to the stress intensity range. There was no significant difference between m for the hydrated old and dehydrated young dentin. In addition to evaluating the fatigue crack growth responses of specimens separately, the cumulative

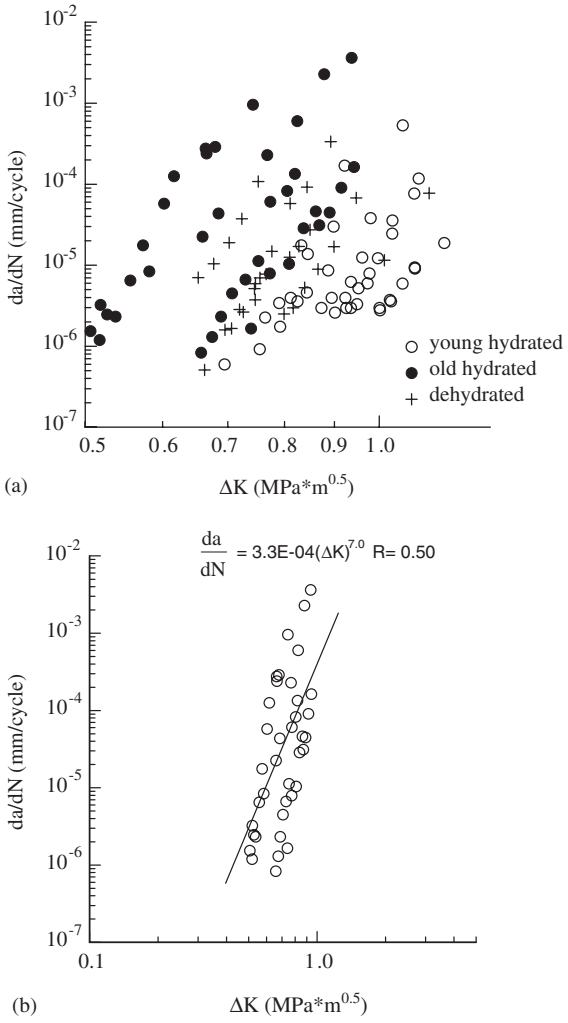

Fig. 5. Fatigue crack growth within human dentin. All experiments were performed with hydration (HBSS) at room temp (22 °C), stress ratio of 0.1 and cyclic load frequency of 5 Hz: (a) complete fatigue crack growth responses for the three groups of dentin specimens. The Paris Law parameters for each individual specimen are listed in Tables 1–3; (b) fatigue crack growth response of the old dentin specimens and power law relationship assuming Paris response. Note the difference in scale used for ΔK from (a).

responses were estimated for each treatment condition by pooling the individual growth responses. An example of the pooled response for the old dentin is shown in Fig. 5(b) and the Paris Law parameters for the pooled growth responses are listed in Table 4. While the old dentin exhibited the largest fatigue crack growth exponent and coefficient of the three conditions, the pooled responses were very different from the average response for each of the three conditions.

An evaluation of the fracture surfaces was conducted using the SEM to identify differences in the structure and mechanisms of fatigue crack extension that contributed to the growth rates. Micrographs from fracture surfaces of young and old hydrated CT specimens are shown in Figs. 6(a) and (b), respectively. These images were obtained from within the Region II growth and present representa-

Table 1
Fatigue crack growth parameters for the young hydrated dentin CT specimens

θ_1 (deg)	Age/gender (years)	C mm/cycle $(MPa\,m^{0.5})^{-m}$	m
90	21/F	0.81E-05	14.3
90	17/M	0.27E-05	13.1
90	34/	0.28E-05	13.6
90	35/M	1.75E-05	13.6
90	21/F	2.02E-05	14.5
90	27/M	1.05E-05	13.1
90	18/M	5.66E-05	11.2
90	30/F	3.99E-05	12.0
90	25/F	31.17E-05	14.0
Average	25	1.76E-05	13.3±1.1

Table 2
Fatigue crack growth parameters for the old hydrated dentin CT specimens

θ_1 (deg)	Age/gender (years)	C mm/cycle $(MPa\,m^{0.5})^{-m}$	m
90	47/F	4.40E-02	29.0
90	50/M	0.18E-02	23.9
90	50/F	0.06E-02	20.7
90	53/F	0.12E-02	15.1
90	52/M	93.0E-02	19.9
90	50/F	22.7E-02	17.4
90	89/M	10.1E-02	28.7
90	50/F	43.0E-02	18.0
Average	55	2.90E-02	21.6±5.2

Table 3
Fatigue crack growth parameters for the young dehydrated dentin CT specimens

θ_1 (deg)	Age/gender (years)	C mm/cycle $(MPa\,m^{0.5})^{-m}$	m
25	19/F	21.0E-03	19.3
45	17/M	0.10E-03	16.8
90	23/F	2.05E-03	20.5
90	19/M	0.31E-03	15.2
90	22/M	0.42E-03	22.0
Average	20	3.55E-03	18.8±2.8

Table 4
Fatigue crack growth parameters estimated from the pooled experimental results for each of the three group of specimens

Group	Age Avg (St. dev.)	C mm/cycle $(MPa\,m^{0.5})^{-m}$	m	R
Young hydrated	25 (7)	1.24 E-05	6.59	0.26
Old hydrated	55 (14)	3.25 E-04	7.05	0.50
Dehydrated	20 (2)	4.96 E-05	6.38	0.25

tive views for the individual conditions. The most distinct difference between the young and old dentin fatigue specimens was found in comparing the peritubular dentin. All the CT specimens from the older patients exhibited partial or complete occlusion of the lumen diameters (Fig. 6(b)). In addition, fracture surfaces of the old dentin appeared much smoother, with far less topographical variation between the planes of failure of the intertubular and peritubular dentin in comparison to the young hydrated dentin. Note that fracture of many of the peritubular cuffs in Fig. 6(a) appear below the fracture surface of the intertubular dentin suggesting that pullout of the peritubular cuffs contributes to energy dissipation during crack extension. Pullout of the peritubular dentin cuffs has been documented in earlier examinations of the fatigue and fracture behavior of dentin [29]. In contrast, the plane of fracture of the peritubular and intertubular components of the old dentin (Fig. 6(b)) appeared more uniformly on the same plane with minimal evidence of pullout. Fracture surfaces of the dehydrated dentin (Fig. 6(c)) exhibited similar features as those for the old dentin with less evidence of peritubular pullout and generally lower apparent surface roughness. At higher magnification, two interesting features were evident on fracture surfaces of the hydrated dentin specimens (Fig. 7). Microcracks were observed in the peritubular cuffs and oriented radially outward from the tubule center. In general, the cracks were found oriented parallel or perpendicular to the direction of crack extension. Both Figs. 7(a) and (b) have been annotated to highlight cracks in the peritubular cuffs. In addition to the microcracks, many of the peritubular cuffs in the hydrated dentin appeared debonded from the surrounding intertubular dentin as highlighted. Microcracks and debonding of the peritubular cuffs were also noticed on the fracture surfaces of the dehydrated dentin, but to a lesser extent. There was no evidence of debonding between the peritubular and intertubular dentin in the old hydrated dentin specimens. Neither was there distinct evidence of microcracking of the peritubular cuffs.

4. Discussion

An evaluation of fatigue crack growth in human dentin was conducted to examine the effects of age and hydration on the crack growth rate and mechanisms of cyclic extension. The average fatigue crack growth exponent (m) for the young hydrated dentin was 13.3 ± 1.1. Nalla et al. [29] examined fatigue crack growth in human dentin and reported an average m of 8.7. This value agrees reasonably well with results of the pooled responses in Table 4 where $6.38 \leqslant m \leqslant 7.05$. The Paris Law exponent has also been determined for fatigue crack growth in bovine dentin ($m = 4.6$) [31,39], bovine bone ($m = 3.7$) [40] and elephant

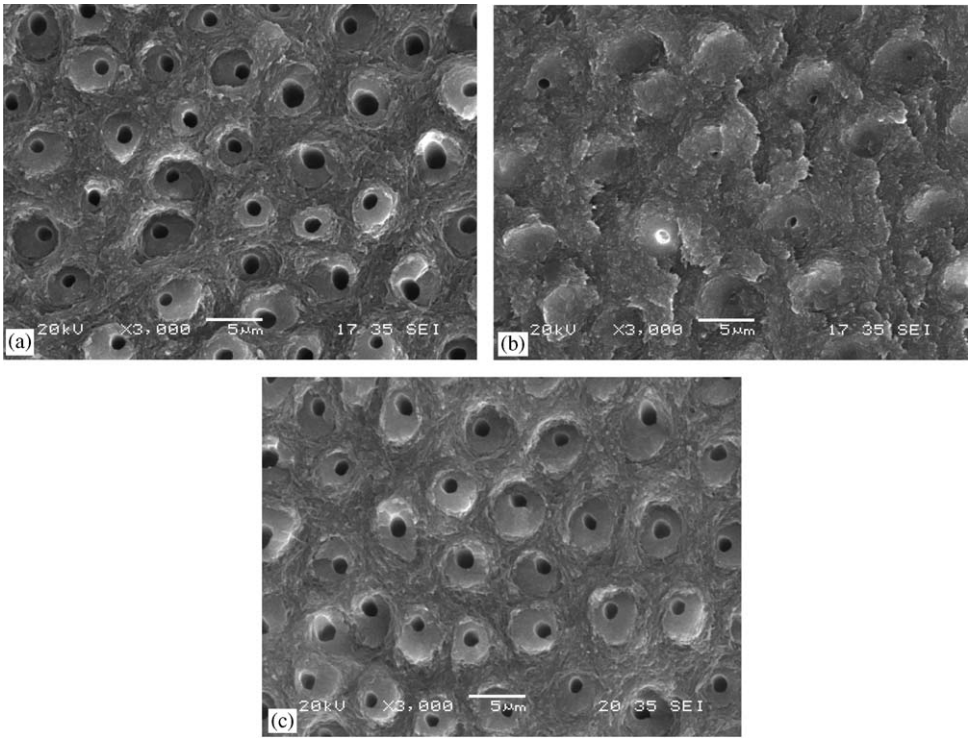

Fig. 6. Typical micrographs from the fatigue fracture surface of young and old dentin CT specimens. The direction of crack growth is from top to bottom in all three micrographs: (a) the fatigue fracture surface from a young hydrated dentin specimen. This dentin is from a female patient 20 years of age. Note the difference in fracture plane of many of the tubules in relation to the intertubular dentin; (b) the fatigue fracture surface from an old hydrated dentin specimen. This dentin is from a male patient 50 years of age. Most of the tubules are occluded and there is very little evidence of peritubular pullout; (c) the fatigue fracture surface from a young dehydrated dentin specimen. This dentin is from a male patient 19 years of age.

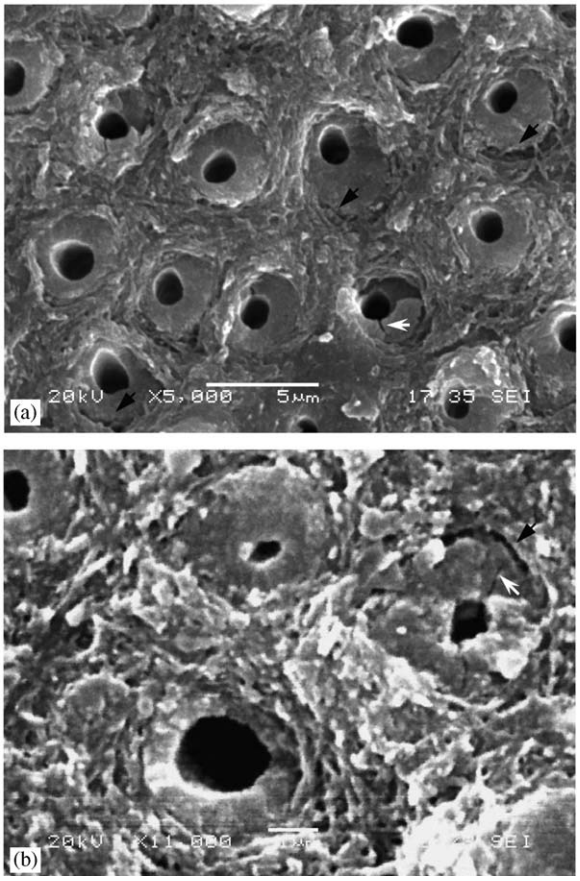

Fig. 7. Additional features of the fatigue crack growth surfaces in the young hydrated dentin. Distinct microcracks were evident in the peritubular cuff (black arrow) and separation between the peritubular and intertubular dentin (white arrow). The direction of crack growth is from top to bottom in each micrograph: (a) specimen from a 20-year-old female patient examined in the hydrated condition; (b) specimen from a 27-year-old patient and was examined in the hydrated condition.

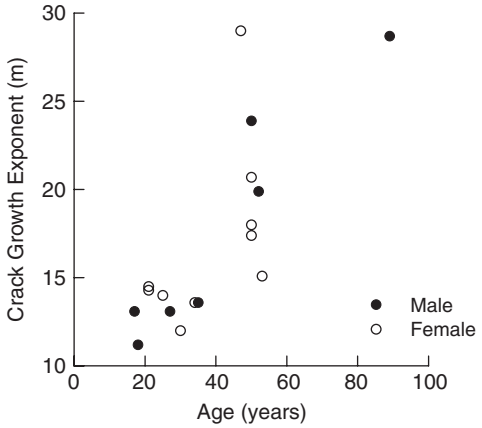

Fig. 8. Distribution of fatigue crack growth exponent (m) with age for the hydrated dentin.

dentin ($12 \leqslant m \leqslant 32$) [41]. While of similar composition, there are differences in structure of these tissues. The tubule density in dentin of bovine molars can be much lower than that of human dentin [31] resulting in differences in the ratio of intertubular and peritubular dentin per unit volume. Similarly, in elephant dentin the peritubular cuffs are less pronounced than in human dentin. The variation in Paris Law exponent for these hard tissues suggests that structure plays an important role on the mechanisms of cyclic crack extension. Interestingly, there is a distinct increase in the growth exponents of the hydrated dentin with respect to age (Fig. 8). While structure is the most obvious contributor to the increase in m with age, changes in the mineral content [19,20], or degradation in the collagen fibril network [42] could also be responsible. Additional study appears necessary to identify the specific structural components resulting in the significant changes in fatigue crack growth resistance of dentin with age.

The stress intensity threshold (ΔK_{th}) for a material represents a critical stress intensity range below which fatigue crack growth is presumed not to occur, or occurs at a very low rate. An approximation for ΔK_{th} of human dentin was recently reported to be 1.06 MPa $m^{0.5}$ [29]. As the crack length was estimated from compliance changes and not measured directly, this quantity is likely an overestimate. Non-linear components of inelastic deformation have been distinguished near the crack tip in dentin and contribute to the local crack opening displacement and macroscopic compliance [24,31]. Region II cyclic crack extension in the human dentin specimens occurred over the range of $0.50 \leqslant \Delta K \leqslant 1.20$ MPa $m^{0.5}$. Though ΔK_{th} was not quantified directly using the standardized approach [30], a first-order estimate, or "apparent" threshold, can be obtained by extrapolating the Region II growth response to an appreciably small growth rate (e.g. 1E-7 mm/cycle). Utilizing this method for the responses in Fig. 5(a) would suggest that the apparent ΔK_{th} for young hydrated dentin is approximately 0.7 MPa $m^{0.5}$. And from a comparison of the cumulative fatigue crack growth responses in this figure there is a decrease in ΔK_{th} with age and dehydration. The apparent ΔK_{th} for both the old and dehydrated dentin appears to be less than 0.6 MPa $m^{0.5}$. It was recently found that there is a decrease in ΔK_{th} and an increase in the fatigue crack growth rate within dentin for increasing stress ratio [39]. Therefore, restorative treatments that result in tensile monotonic stresses in dentin may have additional deleterious effects on older teeth.

Fatigue crack growth in the old and dehydrated dentin occurred more rapidly than within the young hydrated dentin. It is possible to compare the average rate of cyclic growth using the average growth parameters listed in Tables 1–3. For a stress intensity range of 0.9 MPa $m^{0.5}$, the average rate of fatigue crack growth in the young hydrated dentin is 4.4E-6 mm/cycle. In comparison, the average growth rates for the old and dehydrated dentin at the same stress intensity range (ΔK) are 3.0E-3 mm/cycle and 5.0E-4 mm/cycle, respectively. For equivalent driving forces, fatigue crack growth in the old dentin occured at a rate over 100 times that in young hydrated dentin. Dehydration

resulted in an increase in the growth rate of nearly 100 times as well. Differences in musculature and reduction in occlusal forces with age may temper the comparison using an equivalent ΔK. As an alternative, the ΔK required for an average fatigue crack growth rate was estimated. For an average growth rate of 1.0E-5 mm/cycle, the required ΔK is 0.95, 0.69 and 0.73 MPa $m^{0.5}$ for the young and old hydrated dentin and the young dehydrated dentin, respectively.

There was evidence of peritubular cuff pullout in the young hydrated dentin as shown in Fig. 6(a). Fracture surfaces of the old dentin (Fig. 6(b)), and to a lesser extent the dehydrated dentin, showed that pullout was rather uncommon. These observations could suggest that there is relatively weak bonding between the peritubular and intertubular components in young hydrated dentin as evident from debonded peritubular cuffs in Fig. 7. Pullout was not evident in the old dentin, and suggests that the interface is tightly bonded. Perhaps the increase in mineral content of dentin with aging, or redistribution of mineral with dissolution and precipitiation, results in an increase in cohesion between the two constituents, thereby decreasing the relative interfacial sliding with crack growth. There are other potential changes in the mechanisms of energy dissipation associated with dehydration of old dentin that remain to be addressed through additional study.

A previous study estimated the fatigue life of molars with amalgam restorations and adopted the Paris Law parameters for aluminum oxide (Al_2O_3) as a model for dentin [28]. At that time the fatigue properties of dentin were unknown. The fatigue life was defined in terms of the number of years elapsed post-restoration and described in terms of an initial flaw length that resulted from cavity preparation or other restorative process. Cracks as short as 25 μm were estimated to enable tooth fracture within 25 years from the time of restoration. Results from the present study have distinguished that the use of Paris Law parameters for Al_2O_3 to approximate the behavior of human dentin were reasonable for a first-order estimate. However, based on the current understanding of fatigue crack growth in human dentin, results from those numerical evaluations overestimated the fatigue life of restored teeth with flaws. The life would be much less than 25 years. Furthermore, the higher average fatigue crack growth rate in the old dentin (Fig. 5(a)) indicates that cracks introduced within dentin in senior patients during restorative processes would be considerably more detrimental.

Results of the present evaluation represent the first quantitative description for the changes in fatigue crack growth properties of human dentin with age and compare the responses to dehydrated dentin. As with any study there are obvious limitations. The investigation was based on an evaluation of 22 specimens from 22 different patients. Though informative, an evaluation based on a larger population would increase the statistical significance of the findings. Also of importance, the average age of the old dentin was 55, only 30 years higher than the young dentin and well below the lifespan of the average person presently living within the United States and Western Europe. There may be progressive changes in the fatigue properties of dentin that begin with eruption and continue throughout maturation. A study comprised of a more complete distribution of patients and ages could support an evaluation concerning age-specific or age-related trends. Lastly, the dehydrated samples were stored at 60 °C for approximately 5 h. In examinations on the thermostability of human bone [43], these conditions were sufficient to cause denaturation of the collagen fibrils. Although denaturation of collagen has been found to be important to the toughness of bone [44], contributions to the fatigue properties have not been identified. Therefore, the increase in fatigue crack growth rate of the young dehydrated bone may have been partially attributed to denaturation. Despite these limitations, the findings provide additional understanding of the importance of aging to the success of current restorative practices for seniors.

5. Conclusions

An experimental evaluation of the influence from age and dehydration on the fatigue crack growth properties of human dentin was conducted. CT fatigue specimens were prepared from the coronal dentin of third molars extracted from patients with ages that ranged from 17 to 89 years. The specimens were divided into young ($17 \leqslant \text{age} \leqslant 35$) and old ($47 \leqslant \text{age}$) age groups and subjected to Mode I cyclic loading with stress ratio (R) of 0.1. The young dentin was evaluated in both the hydrated and fully dehydrated states whereas the old dentin was examined in the hydrated state only. According to a comparison of fatigue crack growth in the dentin specimens, the following conclusions were drawn:

(1) Overall, Region II fatigue crack growth occurred over a stress intensity range from 0.5 to 1.2 MPa $m^{0.5}$ and with growth rate ranging from 1E-7 to 5E-3 mm/cycle. The highest rate of fatigue crack growth occurred in the old hydrated dentin. For a stress intensity range of 0.9 MPa $m^{0.5}$, the average rate of fatigue crack growth in the young hydrated and young dehydrated dentin was 4.4E-6 mm/cycle and 5.0E-4 mm/cycle, respectively. At the same stress intensity range the average rate of fatigue crack growth in the hydrated old dentin was 3.0E-3 mm/cycle.
(2) The fatigue crack growth exponent for the young hydrated dentin ($m = 13.3 \pm 1.1$) was significantly lower than that for the hydrated old dentin ($m = 21.6 \pm 5.2$; $p < 0.003$) and dehydrated young dentin ($m = 18.8 \pm 2.8$; $p < 0.01$).
(3) The "apparent" stress intensity threshold (ΔK_{th}) for each group of specimens was estimated from an

extrapolation of the steady-state growth rates (Region II). For young hydrated dentin, the apparent stress intensity threshold was approximately $0.7\,\mathrm{MPa\,m^{0.5}}$. Preliminary results suggest that aging results in a reduction in ΔK_{th} occurs with age and may decrease to as low as $0.5\,\mathrm{MPa\,m^{0.5}}$. Thus, fatigue cracks are more likely to initiate from small flaws introduced during cavity preparations and the rate of crack extension is over $100\times$ greater than that in young dentin.

Acknowledgments

The authors gratefully acknowledge support from the Whitaker Foundation in the form of a Biomedical Engineering Research Grant and from the National Science Foundation (BES 0238237). The author A. Nazari also acknowledges support through a GAANN Fellowship.

References

[1] Murray PE, Stanley HR, Matthews JB, Sloan AJ, Smith AJ. Age-related odontometric changes of human teeth. Oral Surg Oral Med Oral Pathol Oral Radiol Endod 2002;93:474–82.
[2] Marcus SE, Drury TF, Brown LJ, Zion GR. Tooth retention and tooth loss in the permanent dentition of adults: United States, 1988–1991. J Dent Res 1996;75:684–95.
[3] Warren JJ, Cowen HJ, Watkins CM, Hand JS. Dental caries prevalence and dental care utilization among the very old. J Am Dent Assoc 2000;131:1571–9.
[4] Weintraub JA, Burt BA. Oral health status in the United States: tooth loss and edentulism. J Dent Ed 1985;49:368–76.
[5] Chiappelli F, Bauer J, Spackman S, Prolo P, Edgerton M, Armenian C, et al. Dental needs of the elderly in the 21st century. Gen Dent 2002;50:358–63.
[6] Pine CM, Pitts NB, Steele JG, Nunn JN, Treasure E. Dental restorations in adults in the UK in 1998 and implications for the future. Br Dent J 2001;190:4–8.
[7] Jones JA, Adelson R, Niesson LC, Gilbert GH. Issues in financing dental care for the elderly. J Public Health Dent 1990;50: 268–75.
[8] Grytten J, Lund E. Future demand for dental care in Norway; a macro-economic perspective. Comm Dent Oral Epidemiol 1999;27:321–30.
[9] Kalsbeek H, Truin GJ, van Rossum GM, van Rijkom HM, Pooterman JH, Verrips GH. Trends in caries prevalence in Dutch adults between 1983 and 1995. Caries Res 1998;32:160–5.
[10] Ten Cate AR. Oral histology. Development structure and function. St Louis, MO: Mosby; 1980.
[11] Carrigan P, Morse DR, Furst ML, Sinai IH. A scanning electron microscopic evaluation of human dentin tubules according to age and location. J Endodont 1984;10:359–63.
[12] Duke ES, Lindemuth J. Variability of clinical dentin substrates. Am J Dent 1991;4:241–6.
[13] Van Meerbeek B, Braem M, Lambrechts P, Vanherle G. Morphological characterization of the interface between resin and sclerotic dentine. J Dent 1994;22(3):141–6.
[14] Prati C, Chersoni S, Mongiorgi R, Montanari G, Pashley DH. Thickness and morphology of the resin infiltrated dentin layer in young, old, and sclerotic dentin. Oper Dent 1999;24:66–72.
[15] Kwong SM, Tay FR, Yip HK, Kei LH, Pashley DH. An ultrastructural study of the application of dentine adhesives to acid-conditioned sclerotic dentine. J Dent 2000;28:515–28.
[16] Tay FR, Kwong SM, Itthagarun A, King NM, Yip HK, Moulding KM, et al. Bonding of a self-etching primer to non-carious cervical sclerotic dentin: interfacial ultrastructure and microtensile bond strength evaluation. J Adhes Dent 2000;2:9–28.
[17] Tay FR, Pashley DH. Resin bonding to cervical sclerotic dentin: a review. J Dent 2004;32:173–96.
[18] Balooch M, Demos SG, Kinney JH, Marshall GW, Balooch G, Marshall SJ. Local mechanical and optical properties of normal and transparent root dentin. J Mater Sci Mater Med 2001;12: 507–14.
[19] Kinney JH, Nalla RK, Pople JA, Breunig TM, Ritchie RO. Age-related transparent root dentin: mineral concentration, crystallite size, and mechanical properties. Biomaterials 2005;26:3363–76.
[20] Porter AE, Nalla RK, Minor A, Jinschek JR, Kisielowski C, Radmilovic V, et al. A transmission electron microscopy study of mineralization in age-induced transparent dentin. Biomaterials 2005;26:7650–60.
[21] Toto PD, Kastelic EF, Duyvejonck KJ, Rapp GW. Effect of age on water content in human teeth. J Dent Res 1971;50:1284–5.
[22] Jameson MW, Hood JA, Tidmarsh BG. The effects of dehydration and rehydration on some mechanical properties of human dentine. J Biomech 1993;26:1055–65.
[23] Kahler B, Swain MW, Moule A. Fracture toughening mechanisms responsible for differences in work of fracture of hydrated and dehydrated dentin. J Biomech 2003;36:229–37.
[24] Kruzic JJ, Nalla RK, Kinney JH, Ritchie RO. Crack blunting, crack bridging and resistance-curve fracture mechanics in dentin: effect of hydration. Biomaterials 2003;24:5209–21.
[25] Huang TJ, Schilder H, Nathanson D. Effects of moisture content and endodontic treatment on some mechanical properties of human dentin. J Endodont 1992;18:209–15.
[26] Tonami K, Takahashi H. Effects of aging on tensile fatigue strength of bovine dentin. Dent Mater J 1997;16:156–69.
[27] Arola D, Reprogel RK. Effects of aging on the mechanical behavior of human dentin. Biomaterials 2005;26:4051–61.
[28] Arola D, Huang MP, Sultan MB. The failure of amalgam dental restorations due to cyclic fatigue crack growth. J Mater Sci Mater Med 1999;10:319–27.
[29] Nalla RK, Imbeni V, Kinney JH, Staninec M, Marshall SJ, Ritchie RO. In vitro fatigue behavior of human dentin with implications for life prediction. J Biomed Mater Res 2003;66A:10–20.
[30] ASTM E647. Standard test method for measurement of fatigue crack growth rates. In: Annual book of ASTM standards. Philadelphia, PA: American Society for Testing and Materials; 2000.
[31] Arola D, Rouland JA, Zhang D. Fatigue and fracture of bovine dentin. Exp Mech 2002;42:380–8.
[32] Nalla RK, Kinney JH, Ritchie RO. Effect of orientation on the in vitro fracture toughness of dentin: the role of toughening mechanisms. Biomaterials 2003;24:3955–68.
[33] Paris PC, Erdogan F. A critical analysis of crack propagation laws. J Basic Eng 1963;D85:528–34.
[34] Iwamoto N, Ruse Dorin N. Fracture toughness of human dentin. J Biomed Mater Res 2003;66:507–12.
[35] Arola D, Rouland JA. The effects of tubule orientation on fatigue crack growth in dentin. J Biomed Mater Res 2003;67A:78–86.
[36] Zienkiewicz OC, Emson C, Bettess P. A novel boundary infinite element. Int J Num Methods Eng 1983;19:393–404.
[37] Kinney JH, Marshall SJ, Marshall GW. The mechanical properties of human dentin: a critical review and re-evaluation of the dental literature. Crit Rev Oral Biol Med 2003;14:13–29.
[38] Anderson TL. Fracture mechanics: fundamentals and applications. Boca Raton, FL: CRC Press; 1991.
[39] Arola D, Zheng W, Sundaram N, Rouland JA. Stress ratio contributes to fatigue crack growth in dentin. J Biomed Mater Res 2005;73A:201–12.
[40] Wright TM, Hayes WC. The fracture mechanics of fatigue crack propagation in compact bone. J Biomed Mater Res 1976;7: 637–48.

[41] Kruzic JJ, Nalla RK, Kinney JH, Ritchie RO. Mechanistic aspects of in vitro fatigue crack growth in dentin. Biomaterials 2005;26: 1195–204.

[42] Pashley DH, Tay FR, Yiu C, Hashimoto M, Breschi L, Carvalho RM, et al. Collagen degradation by host-derived enzymes during aging. J Dent Res 2004;83:216–21.

[43] Li X, Agrawal CM, Wang X. Age dependence of in situ thermostability of collagen in human bone. Calcif Tissue Int 2003;72: 513–8.

[44] Wang X, Bank RA, TeKoppele JM, Hubbard GB, Athanasiou KA, Agrawal CM. Effects of collagen denaturation on the toughness of bone. Clin Orthop Relat Res 2000;371:228–39.